Available online at www.sciencedirect.com
SCIENCE DIRECT®
International Journal of Heat and Mass Transfer 48 (2005) 1164–1174
International Journal of HEAT and MASS TRANSFER
www.elsevier.com/locate/ijhmt

# Effects of heat source distribution on natural convection induced by internal heating

Yuji Tasaka *, Yasushi Takeda

*Division of Mechanical Science, Graduate School of Engineering, Hokkaido University, Kita-13 Nishi-8, Sapporo 060-8628, Japan*

Received 9 July 2004
Available online 8 December 2004

**Abstract**

The effects of a heat source distribution on natural convection induced by internal heating are studied by using simplified models of the distribution. A linear stability analysis is made to study the effects on critical Rayleigh number and critical wavenumber. The total amount of heat generation to set convection and the asymmetry in the convective motion are discussed for two extreme cases of heat source distribution. Effect of additional bottom wall heating is also investigated on the critical condition and the asymmetry of the convective motion.


*Keywords:* Natural convection; Distributed internal heat generation; Stability analysis; Symmetry of velocity profile

## 1. Introduction

Natural convection occurring in nature and some industrial devices are driven by internal heating. Examples in nature include mantle convection in the Earth [1–4], and motions in the Earth and Venusian atmospheres [5,6]. In the artificial structures, microwave ovens and induction heater such as an electric melter generate internal heat. In the event of hypothetical core meltdown of the nuclear reactor heat generation is internal. Furthermore, heat generation in the above configurations is non-uniform. In the atmosphere, sunlight is absorbed more strongly in the upper layer. Also for the induction heating by passing electric current, heat generation is concentrated more in the outer layer of a heating material. This effect has been almost neglected although internal heating changes convective motion drastically.

Despite the importance of internal heat generation, there are few systematic investigations of its effects. Most of previous works have only considered the much simpler case of uniform heat generation. For example, Tritton and Zarraga [7] and Schwiderski and Schwab [8] carried out experimental investigations and found various interesting features; of particular interest was the dilatation of convection cells with increasing rate of internal heat generation. Theoretical studies by Roberts [9], Tveitereid and Palm [10] and Tveitereid [11], however, could not clarify this phenomenon. They attributed the cell dilatation to non-uniform heat generation due to imperfections in the experiments; that is, a deviation from uniform heating due to a spatially varying electrical conductivity (an improved and more precise experimental investigation is under progress by us [12]).

Non-uniform distribution of internal heat generation was treated by Krishnamurti [6] in the context of cloud

* Corresponding author. Tel.: +81 11 706 6373; fax: +81 11 706 7889.
*E-mail address:* tasaka@ring-me.eng.hokudai.ac.jp (Y. Tasaka).

0017-9310/$ - see front matter © 2004 Elsevier Ltd. All rights reserved.
doi:10.1016/j.ijheatmasstransfer.2004.09.044

**Nomenclature**

| | | | |
|---|---|---|---|
| $c_p$ | specific heat | $\boldsymbol{u}(u,v,w)$ | velocity vector and its components |
| $g$ | gravity | $\boldsymbol{x}(x,y,z)$ | coordinates of position |
| $H$ | volumetric heat source | $\beta$ | bulk modulus |
| $H_0$ | total power deposited | $\Delta T$ | temperature difference between the top and the bottom boundaries |
| $k$ | horizontal wavenumber | | |
| $L$ | height of the fluid layer | $\varepsilon$, $\eta$ | characteristic length of heat source distribution |
| $p$ | pressure | | |
| $Pr$ | Prandtl number | $\Theta$ | $R_I/R$ |
| $q$ | distribution function of internal heat source | $\kappa$ | thermal diffusivity |
| $R_I$ | internal Rayleigh number | $\lambda$ | thermal conductivity |
| $R$ | external Rayleigh number | $\mu$ | viscosity |
| $t$ | time | $\nu$ | dynamic viscosity |
| $T$ | temperature | $\rho$ | density |
| * | dimension variable | ~ | amplitude function of perturbation |
| ^ | perturbation | c | critical value |
| ⁻ | stationary value | 1 | value at $T = T_1$ |

formation in meteorology. Her experiment, however, uses a chemical reaction to simulate the internal heat generation and cannot be easily modeled for analysis. Yücel and Bayazitoglu [13] also investigated a non-uniform distribution theoretically by using a model in which the heat source increases exponentially from the lower to the upper boundary. Their model, however, was combined with complex boundary conditions which consequently did not allow the fundamental characteristics of heat source distribution to be clarified.

In the present investigation, we focus our study on the influence of the heat source distribution on the convection. As we consider that most of the distribution of the internal heating is caused by absorption of radiating wave such as microwave, an exponential distribution in the vertical direction is assumed. Using a linear stability analysis, we investigated two cases. In Section 3 we consider the case where the heat source is concentrated near the bottom or the top boundary. Earlier studies in 1970s [7–9] (as well as in our investigations [12]) adopted an adiabatic boundary condition at the bottom. In Section 4 we relax this constraint and investigate the non-adiabatic case where the bottom boundary is maintained at a constant temperature (wall heating). This problem might be called "mixed convection" (mixture of Rayleigh–Bénard Convection and internal heat source convection).

## 2. Basic equations with uniform internal heating

A horizontal fluid layer unbound for the horizontal directions has steady internal heat generation $H(z^*)$ as shown in Fig. 1. Let a top ($z^* = L$) and a bottom ($z^* = 0$) boundary be isothermal with the temperature

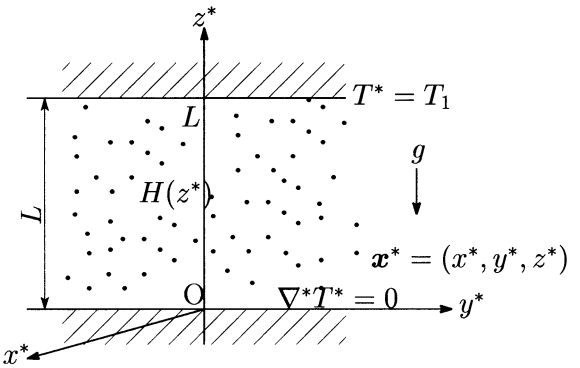


Fig. 1. Coordinates and configuration; thermal boundary conditions at the top and bottom are isothermal and adiabatic respectively, internal heat source $H$ distributes in the vertical direction.

$T^* = T_1$ and adiabatic, $\nabla^* T^* = 0$, respectively. Following assumptions are made: a temperature field is dominated by heat conduction and by internal heating in stationary state, and a pressure field $p^*(\boldsymbol{x}^*)$ is in hydrostatic equilibrium. The fluid layer obeys Boussinesq approximation, and density $\rho^*$ is a linear function of temperature independently of pressure.

Basic equations in the fluid field (velocity $\boldsymbol{u}^*$, $p^*$, $T^*$ and $\rho^*$) are the continuity equation, the equation of motion, the energy equation and the equation of state, as follows.

$$\nabla^* \cdot \boldsymbol{u}^* = 0, \tag{1}$$

$$\rho_1 \frac{D\boldsymbol{u}^*}{Dt^*} = -\nabla^* p^* - \rho^* g \boldsymbol{e}_z + \mu \Delta^* \boldsymbol{u}^*, \quad \boldsymbol{e}_z = (0,0,1), \tag{2}$$

$$\rho_1 c_p \frac{DT^*}{Dt^*} = \lambda \Delta^* T^* + H(z^*), \tag{3}$$

$$\rho^* = \rho_1[1 - \beta(T^* - T_1)], \tag{4}$$

where Laplacian $\Delta^* = \partial^2/\partial x^{*2} + \partial^2/\partial y^{*2} + \partial^2/\partial z^{*2}$. Physical properties $\lambda$, $\mu$, $\beta$, $H$ and $c_p$ are thermal conductivity, viscosity, bulk modulus ($\beta = (dV/dT^*)_{T_1}/V$, $V$ is volume), amount of heat generation per unit time and per unit volume and specific heat respectively. In addition, $\rho_1 = \rho(T_1)$. It is assumed that temperature dependence in these physical properties can be neglected.

At first uniform internal heating $H(z^*) = H_0$ is considered. In a stationary state ($\bar{\boldsymbol{u}} = 0$), solutions of Eqs. (2)–(4) are

$$\overline{T}^* - T_1 = \frac{H_0}{2\lambda}(L^2 - z^{*2}), \tag{5}$$

$$\bar{\rho}^* = \rho_1\left[1 - \beta\frac{H_0}{2\lambda}(L^2 - z^{*2})\right], \tag{6}$$

$$\bar{p}^* = \rho_1 g z^*\left[1 - \beta\frac{H_0}{2\lambda}\left(L^2 - \frac{1}{3}z^{*2}\right)\right] + \text{const.} \tag{7}$$

By defining perturbations as $\hat{\boldsymbol{u}}^*$, $\widehat{T}^*$, $\hat{\rho}^*$ and $\hat{p}^*$, physical variables can be expressed as

$$\boldsymbol{u}^* = \hat{\boldsymbol{u}}^*, \quad T^* = \overline{T}^* + \widehat{T}^*, \quad \rho^* = \bar{\rho}^* + \hat{\rho}^*, \quad p^* = \bar{p}^* + \hat{p}^*.$$

Equations (1)–(4) are transformed by substituting these definitions and Eqs. (5) and (6), and are linearized. We define dimensionless physical variables as

$$\boldsymbol{x} = \frac{\boldsymbol{x}^*}{L}, \quad t = \frac{\kappa_1}{L^2}t^*, \quad p = \frac{p^* L^2}{\rho_1 \kappa_1^2}, \quad \boldsymbol{u} = \frac{L}{\kappa_1}\boldsymbol{u}^*, \tag{8}$$

where thermal diffusivity $\kappa_1 = \lambda/(\rho_1 c_p)$. By using temperature difference between the top and the bottom boundary, $\Delta T \equiv T_0 - T_1 = H_0 L^2/(2\lambda)$, dimensionless temperature is defined as

$$T = \frac{1}{\Delta T}T^*. \tag{9}$$

Finally linearized equations become

$$\nabla \cdot \hat{\boldsymbol{u}} = 0, \tag{10}$$

$$\frac{\partial \hat{\boldsymbol{u}}}{\partial t} = -\nabla \hat{p} + R_1 Pr \widehat{T}\boldsymbol{e}_z + Pr\Delta\hat{\boldsymbol{u}}, \quad \boldsymbol{e}_z = (0,0,1), \tag{11}$$

$$\frac{\partial \widehat{T}}{\partial t} + \frac{d\overline{T}}{dz}\hat{w} = \Delta\widehat{T}, \tag{12}$$

where

$$\left.\begin{aligned} Pr &= \frac{\nu_1}{\kappa_1}\left(= \frac{\mu/\rho_1}{\kappa_1}\right): \text{Prandtl number},\\ R_1 &= \frac{g\beta H_0 L^5}{2\lambda\nu_1\kappa_1}: \text{Rayleigh number}. \end{aligned}\right\} \tag{13}$$

Being distinct from usual Rayleigh number related with wall heating (external Rayleigh number), this kind of Rayleigh number is called an internal Rayleigh number.

Perturbations are described as

$$\begin{bmatrix} \hat{\boldsymbol{u}}(\boldsymbol{x},t) \\ \widehat{T}(\boldsymbol{x},t) \\ \hat{p}(\boldsymbol{x},t) \end{bmatrix} = \begin{bmatrix} \tilde{\boldsymbol{u}}(z) \\ \widetilde{T}(z) \\ \tilde{p}(z) \end{bmatrix} \exp[\mathrm{i}(\alpha_x x + \alpha_y y) + \sigma t]. \tag{14}$$

By substituting this formula into Eqs. (10)–(12), perturbation equations are derived as

$$\left(\frac{d^2}{dz^2} - k^2 - \frac{\sigma}{Pr}\right)\left(\frac{d^2}{dz^2} - k^2\right)\tilde{w} = R_1 k^2 \widetilde{T}, \tag{15}$$

$$\left(\frac{d^2}{dz^2} - k^2 - \sigma\right)\widetilde{T} = \frac{d\overline{T}}{dz}\tilde{w}, \tag{16}$$

where $k$ is horizontal wavenumber, $k = \sqrt{\alpha_x^2 + \alpha_y^2}$.

Boundary conditions for perturbation velocity are derived from rigid boundary condition as

$$\tilde{w} = \frac{d\tilde{w}}{dz} = 0 \quad \text{at } z = 0, 1. \tag{17}$$

Corresponding to adiabatic boundary ($z = 0$) and isothermal boundary ($z = 1$), boundary conditions for temperature are

$$\frac{d\widetilde{T}}{dz} = 0 \text{ at } z = 0, \quad \widetilde{T} = 0 \quad \text{at } z = 1. \tag{18}$$

Linear stability analysis is made on perturbation Eqs. (15) and (16) with boundary conditions (17) and (18). Critical values, the critical Rayleigh number $R_c$ and critical wavenumber $k_c$, for uniform internal heating calculated by Roberts [9] are $R_c = 1386.14$ and $k_c = 2.629$ (Roberts used the definition of internal Rayleigh number as $R_I = (g\beta H L^5)/(\lambda\nu\kappa)$, and it is twice in our definition. Thus, $R_c$ in his paper is 2772.28). Comparing with Rayleigh–Bénard convection ($R_c = 1707.76$ and $k_c = 3.117$, Reid and Harris [14]), these results show that convection occurs more easily and convection cell becomes larger in the internally heated convection.

## 3. Distributed heat source

### 3.1. General treatment of heat source distribution

Distributed internal heat source is expressed as follows.

$$H(z,\varepsilon) = \frac{H_0}{\varepsilon}q(z,\varepsilon), \tag{19}$$

where, $q(z,\varepsilon)$ is a normalized function that expresses a form of the heat source distribution, and $\varepsilon$ is a characteristic length related to the form.

By this definition,

$$\int_0^1 H(z,\varepsilon)\,\mathrm{d}z = H_0.$$

$H_0$ is total power induced by internal heating without dependence on a distribution form. In the case with uniform internal heating, heat source distribution can be expressed by this formula as $q(z,\varepsilon)/\varepsilon = 1$.

### 3.2. Concentration of heat source on the bottom boundary

Heat source distribution, which concentrates near the bottom boundary, is considered. A model of heat source distribution, which has the maximum at the bottom and decreases to the upward direction exponentially as follows, is used.

$$H(z,\varepsilon) = \frac{H_0}{Q(\varepsilon)}\exp\left(-\frac{z}{\varepsilon}\right), \tag{20}$$

$$Q(\varepsilon) = \int_0^1 \exp\left(-\frac{z}{\varepsilon}\right)\mathrm{d}z = \varepsilon\left[1-\exp\left(-\frac{1}{\varepsilon}\right)\right].$$

Heat source distributions for various values of $\varepsilon$ are shown in Fig. 2. As is seen in this figure, heat source concentrates more near the bottom with decrease of $\varepsilon$. It becomes close to uniform distribution by increasing $\varepsilon$. $H$ becomes $H_0$ when $\varepsilon$ approaches the limit of infinity. For this model of heat source distribution, the temperature profile in heat conduction is derived by integrating the equation of heat conduction (3), which contains the distribution (20), with boundary conditions (18) as follows.

$$\overline{T}^* - T_1 = \frac{H_0 L^2}{\lambda}\frac{\varepsilon^2}{Q(\varepsilon)}\left[\exp\left(-\frac{1}{\varepsilon}\right) - \exp\left(-\frac{z}{\varepsilon}\right) + \frac{1-z}{\varepsilon}\right]. \tag{21}$$

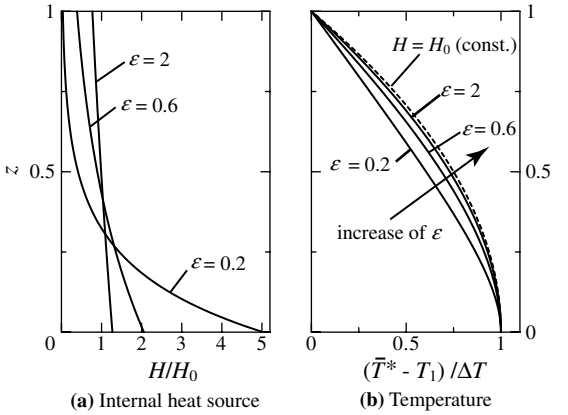


Fig. 2. (a) heat source distribution and (b) temperature profile at conduction state versus $\varepsilon$, broken line shows temperature profile for uniform internal heating, $H = H_0$.

A temperature difference between the top and the bottom, $\Delta T$, is

$$\Delta T = \overline{T}^*(z=0) - T_1 = \frac{H_0 L^2}{\lambda}\frac{\varepsilon^2}{Q(\varepsilon)}\left[\exp\left(-\frac{1}{\varepsilon}\right) + \frac{1-\varepsilon}{\varepsilon}\right]. \tag{22}$$

Temperature profile for the vertical direction expressed by Eq. (21) is shown in Fig. 2(b). In this figure a broken line shows a profile in the case with uniform heating; namely $H = H_0$. $\overline{T}^*$ approaches this curve asymptotically with respect to $\varepsilon$. Fig. 3 shows a variation of the normalized temperature difference $\Delta T/(H_0L^2/2\lambda)$ as a function of $\varepsilon$, where the demoninator is the temperature difference for uniform heating, $H = H_0$. At $\varepsilon = 0$, $\Delta T$ is two times the temperature difference for uniform heating, and the limiting value for $\varepsilon \to \infty$ is equal to the value at uniform heating.

Perturbation equation on temperature for such internal heat distribution is derived as

$$\left(\frac{\mathrm{d}^2}{\mathrm{d}z^2} - k^2 - \sigma\right)\tilde{T} = -\frac{1}{C(\varepsilon)}\left[1-\exp\left(-\frac{z}{\varepsilon}\right)\right]\tilde{w}, \tag{23}$$

where

$$C(\varepsilon) = \varepsilon\left[\exp\left(-\frac{1}{\varepsilon}\right) + \frac{1}{\varepsilon} - 1\right].$$

For the perturbation equation (15), the internal Rayleigh number is defined as

$$R_\mathrm{I} = \frac{g\beta H_0 L^5}{\lambda\nu_1\kappa_1}\frac{\varepsilon^2}{Q(\varepsilon)}\left[\exp\left(-\frac{1}{\varepsilon}\right) + \frac{1}{\varepsilon} - 1\right]. \tag{24}$$

$R_\mathrm{I}$ has a characteristic length of heat source distribution $\varepsilon$ in addition to the height of the fluid layer $L$.

In a state of neutral stability ($\sigma = 0$) an equation for $\tilde{w}$ is derived from Eqs. (15) and (23) as

$$\left(\frac{\mathrm{d}^2}{\mathrm{d}z^2} - k^2\right)^3\tilde{w} = -\frac{R_\mathrm{I}k^2}{C(\varepsilon)}\left[1-\exp\left(-\frac{z}{\varepsilon}\right)\right]\tilde{w}. \tag{25}$$

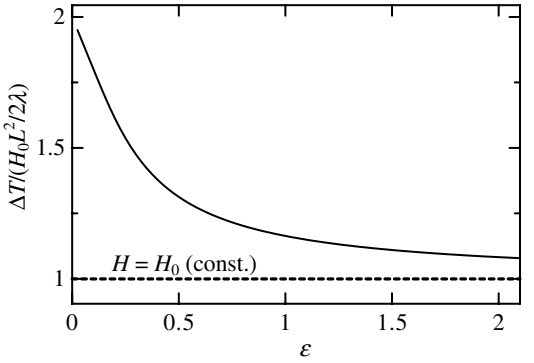


Fig. 3. Variation of normalized temperature difference $\Delta T/(H_0L^2/2\lambda)$ versus $\varepsilon$, where the denominator is temperature difference for uniform heating $H = H_0$.

The method used in Sparrow et al. [15] and Kulacki and Goldstein [16] calculated eigenvalues. A solution of Eq. (25) is expressed by using power series as following:

$$\tilde{w} = \sum_{i=0}^{5} C_i f^{(i)}(z), \quad f^{(i)} = \sum_{n=0}^{\infty} b_n^{(i)} z^n. \tag{26}$$

A characteristic equation is derived using this solution, perturbation equation (25) and boundary conditions (17) and (18). Derivation of characteristic equation is shown in Sparrow et al. [15]. The method of determining $b_n^{(i)}$ will be shown in Appendix.

Critical values, $R_c$ and $k_c$, for several values of $\varepsilon$ were obtained. Variations in these values with respect to $\varepsilon$ are shown in Fig. 4. In these figures, broken lines show critical values for uniform internal heating calculated by Roberts [9]. $R_c$ and $k_c$ increase with $\varepsilon$ and approach asymptotically to these lines; $H = H_0$. The largest difference of $k_c$ from uniform heating is only 2% for $\varepsilon$ investigated here, so that this distribution of heat source has little influence on the size of convection cell. On the other hand, $R_c$ for $\varepsilon = 0.2$ is 13% smaller than that for uniform heating. Therefore the concentration of heat source near the bottom would lower the stability of the convection.

Discussing total power necessary to induce convection is also important for a laboratory experiment and for industrial problems related with heat removing. A part of $R_c$ related to the form of heat source distribution is expressed as

$$D(\varepsilon) \equiv \frac{\varepsilon^2}{Q(\varepsilon)}\left[\exp\left(-\frac{1}{\varepsilon}\right) + \frac{1}{\varepsilon} - 1\right].$$

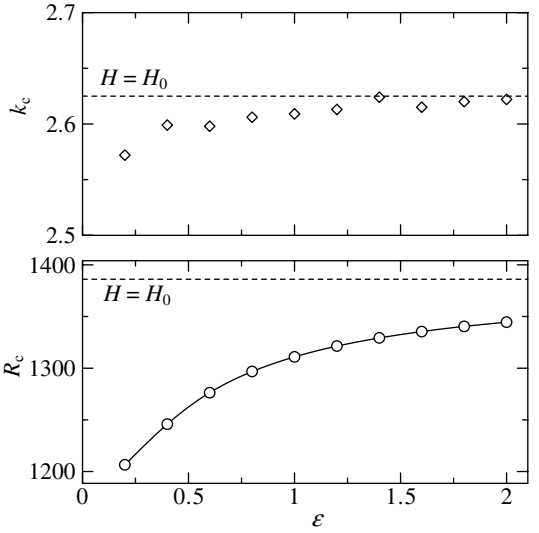


Fig. 4. Variation of critical Rayleigh number $R_c$ (below) and critical wavenumber $k_c$ (above) versus $\varepsilon$, broken lines express $k_c$ and $R_c$ for uniform internal heating.

Because $R_c/D(\varepsilon) \sim H_0$, comparison of total power in each case is equal to estimating $R_c/D(\varepsilon)$. Fig. 5 shows the variation of total power with respect to $\varepsilon$. In $\varepsilon = 2$, convection occurs at smaller heat power than that in uniform heating by 10% in spite of the temperature profile in $\varepsilon = 2$ being nearly that in uniform heating as shown in Fig. 2(b). This result suggests that such slight concentration of heat source to the bottom can promote convection occurring significantly without increasing total heat amount as an advantage, and also slight deviation of heat source from uniform heating induces large difference of the critical Rayleigh number even the same amount of heat is added to the fluid layer.

### 3.3. Concentration of heat source on the top boundary

A heat source distribution in which heat source concentrates on the top boundary is expressed as

$$H(z,\eta) = \frac{H_0}{Q(\eta)} \exp\left(\frac{z-1}{\eta}\right), \tag{27}$$

where

$$Q(\eta) = \int_0^1 \exp\left(\frac{z-1}{\eta}\right) \mathrm{d}z = \eta\left[1 - \exp\left(-\frac{1}{\eta}\right)\right].$$

It becomes the maximum at the top boundary. In this definition, $\eta$ is a characteristic length of the heat source distribution, and as shown in Fig. 6(a), heat amount more concentrates on the top boundary with decrease of $\eta$.

Temperature profile in the conduction state for this heat source distribution and temperature difference are derived as

$$\overline{T}^* - T_1 = \frac{H_0 L^2}{\lambda}\frac{\eta^2}{Q(\eta)}\left[1 - \exp\left(\frac{z-1}{\eta}\right) + \frac{z-1}{\eta}\exp\left(-\frac{1}{\eta}\right)\right], \tag{28}$$

and

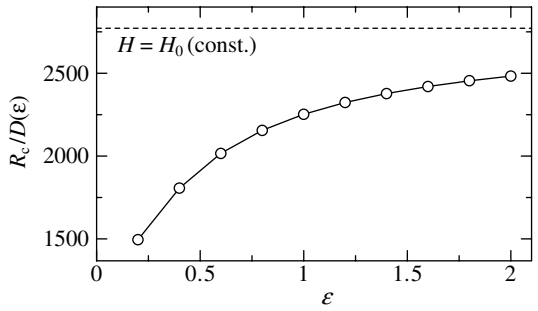


Fig. 5. Variation of total power necessary to induce convection with respect to $\varepsilon$, broken line shows one for uniform internal heating.

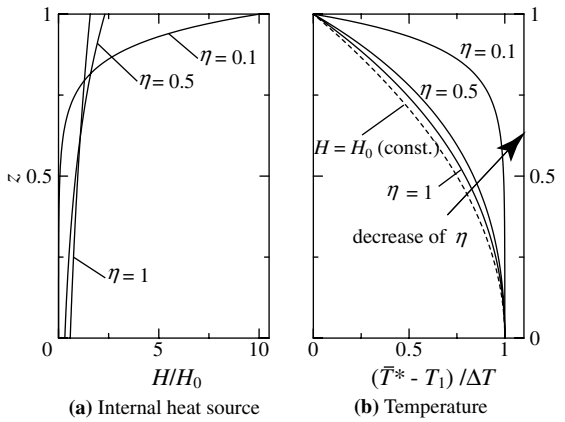


Fig. 6. (a) heat source distribution and (b) temperature profile at conduction state versus $\eta$, broken line shows temperature profile for uniform internal heating, $H = H_0$.

$$\Delta T = \overline{T}^{*}(z=0) - T_1 = \frac{H_0 L^2}{\lambda}\frac{\eta^2}{Q(\eta)}\left[1 - \left(1+\frac{1}{\eta}\right)\exp\left(-\frac{1}{\eta}\right)\right]. \quad (29)$$

Fig. 6(b) shows temperature profile expressed as Eq. (28) for a several value of $\eta$. For small $\eta$, temperature variation exists only near the top and slightest near the bottom. For instance, at $\eta = 0.1$, temperature is nearly constant in the lower half of the fluid layer and decreasing amount of temperature at $z = 0.5$ is only 1% or less of the maximum. Fig. 7 shows a variation of the normalized temperature difference $\Delta T/(H_0 L^2/2\lambda)$ as a function of $\eta$. It converges to the temperature difference for uniform heating at the limit of $\eta \to \infty$ and becomes zero at $\eta = 0$.

From Eqs. (16), (28) and (29), the perturbation equation is derived as follow.

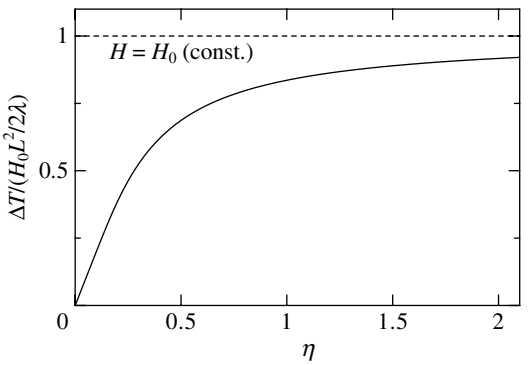


Fig. 7. Variation of normalized temperature difference $\Delta T/(H_0 L^2/2\lambda)$ versus $\eta$, where the denominator is temperature difference for uniform heating $H = H_0$.

$$\left(\frac{d^2}{dz^2} - k^2 - \sigma\right)\tilde{T} = -\frac{1}{E(\eta)}\left[\exp\left(\frac{z-1}{\eta}\right) - \exp\left(-\frac{1}{\eta}\right)\right]\tilde{w}, \quad (30)$$

where

$$E(\eta) = \eta\left[1 - \left(1+\frac{1}{\eta}\right)\exp\left(-\frac{1}{\eta}\right)\right].$$

On the other hand, from Eq. (15),

$$\left(\frac{d^2}{dz^2} - k^2 - \frac{\sigma}{Pr}\right)\left(\frac{d^2}{dz^2} - k^2\right)\tilde{w} = R_1 k^2 \tilde{T}, \qquad R_1 = \frac{g\beta H_0 L^5}{\lambda \nu_1 \kappa_1}\frac{\eta^2}{Q(\eta)}\left[1 - \left(1+\frac{1}{\eta}\right)\exp\left(-\frac{1}{\eta}\right)\right]. \quad (31)$$

The equation for perturbation velocity $\tilde{w}$ in the state of neutral stability ($\sigma = 0$) is

$$\left(\frac{d^2}{dz^2} - k^2\right)^3 \tilde{w} = -\frac{R_1 k^2}{E(\eta)}\left[\exp\left(\frac{z-1}{\eta}\right) - \exp\left(-\frac{1}{\eta}\right)\right]\tilde{w}. \quad (32)$$

Fig. 8 shows variations of $R_c$ and $k_c$ with respect to $\eta$. Both variations are gradual for $\eta \geqslant 0.5$, but sharp below $\eta = 0.5$. At $\eta = 0.1$, for instance, $R_c$ becomes 4.5 times as large as that for $H = H_0$. For a small value of $\eta$, the temperature is nearly constant over a wide range of the vertical direction as seen in Fig. 6(b). Temperature gradient is gradual, but the fluid layer is certainly unstable just only gradual temperature gradient. Such a layer, however, clearly reduces instability of the fluid layer as given in Fig. 8. Therefore, we name such a layer as a

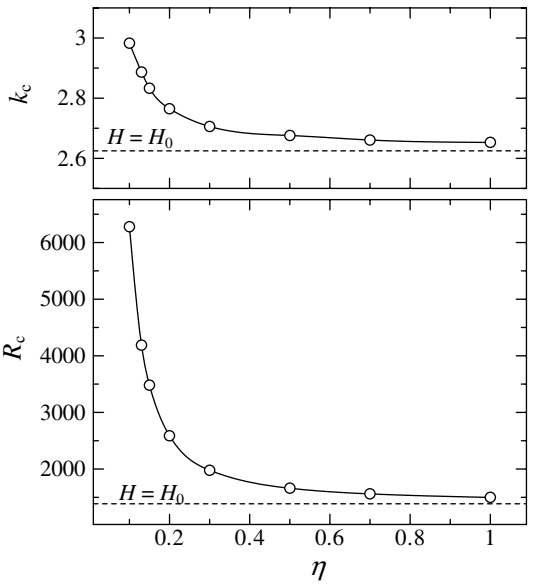


Fig. 8. Variation of critical Rayleigh number $R_c$ (below) and critical wavenumber $k_c$ (above) versus $\eta$, broken lines express $k_c$ and $R_c$ for uniform internal heating.

quasi-stable layer. Large deformation of a temperature profile from uniform heating with formation of the quasi-stable layer especially increases a dimensionless critical wavenumber $k_c$. The increase of $k_c$ from uniform heating is approximately 14% at $\eta = 0.1$, and an extreme concentration of heat source on the bottom boundary may induce large influence on the size of the convection cell.

Eigenfunction $\tilde{w}$ for uniform internal heating is almost symmetrical with respect to the half line of the fluid layer. For a heat source distribution in which heat source concentrates on the top boundary, $\tilde{w}$ is not symmetric and the center of the convection cells becomes slightly higher than the half line. For instance, this distance is approximate 3% of the height of the fluid layer for the distributed internal heat source with $\eta = 0.1$. Profile of $\tilde{w}$ in the internally heated convection is originally asymmetric because temperature profile in the conduction state is asymmetric being different from the standard Rayleigh–Bénard convection. It is, however, not apparent in the uniform internal heating. Concentration of heat source on the top boundary enhances such asymmetric property of $\tilde{w}$. There is no clear critical value of $\eta$ for asymmetry to be induced and thickness of the quasi-stable layer cannot be determined because temperature decreases to the vertical direction monotonically even for small value of $\eta$.

Using $R_c/D(\eta)$ can estimate total power necessary to induce convection, where

$$D(\eta) = \frac{\eta^2}{Q(\eta)}\left[1 - \left(1 + \frac{1}{\eta}\right)\exp\left(-\frac{1}{\eta}\right)\right].$$

Fig. 9 shows a variation of such total power with respect to $\eta$. When $\eta = 0.1$, the fluid layer needs larger heating power than in uniform heating by 20 times. Even at $\eta = 1$, the total power becomes 1.3 times.

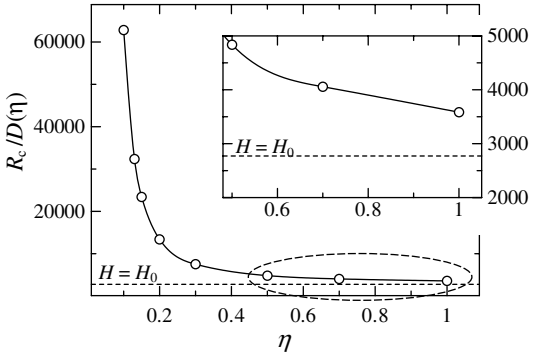


Fig. 9. Variation of total power necessary to induce convection with respect to $\eta$, broken line shows one for uniform internal heating. Inside figure shows closeup of part enclosed by broken curve.

## 4. Combination with wall heating

In the last section we neglected heat flow through the bottom boundary in order to estimate influence of distributed internal heat source on an experiment, which has adiabatic boundary as the bottom boundary. In this section we consider the case in which there is wall heating at the bottom with $T^* = T_2$, $T_2 > T_1$ not only internal heating as more realistic problem.

### 4.1. Temperature profile with Internal and External Rayleigh number

Adding of wall heating to the internally heated convection changes a form of a temperature profile. Temperature in the conduction state $\overline{T}^*$ is derived as

$$\overline{T} \equiv \frac{\overline{T}^* - T_1}{T_2 - T_1} = -\Theta z^2 + (\Theta - 1)z + 1,$$
$$\text{where } \Theta = \frac{H_0 L^2}{2\lambda(T_2 - T_1)}. \tag{33}$$

$\Theta$ is a dimensionless parameter, which determines a form of a temperature profile. Fig. 10 shows examples of temperature profile for two values of $\Theta$. For $\Theta \leqslant 1$, the temperature profile written by a broken line has fully unstable gradient, namely, temperature decreases to the vertical direction monotonically. On the contrary, for $\Theta > 1$, the profile written by a solid line has a local stable layer in which temperature gradient is positive with dimensionless height $h_s$. It is easy to derive from Eq. (33) that $h_s = (\Theta - 1)/2\Theta$. $h_s$ increases with respect to $\Theta$ and $h_s$ becomes 1/2 at $\Theta \to \infty$.

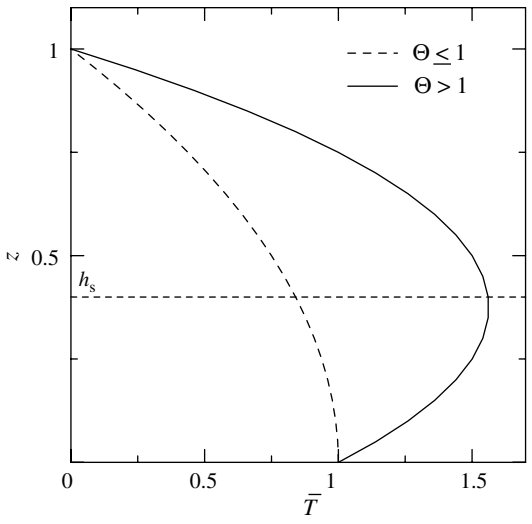


Fig. 10. Comparison of temperature profiles for difference $\Theta$; solid line $\Theta \leqslant 1$ and broken line $\Theta > 1$. $h_s$ shows height of local stable layer in which temperature gradient is positive in the vertical direction.

The definition of $\Theta$ is represented as

$$\Theta = \frac{H_0 L^2}{2\lambda}/(T_2 - T_1), \\ = \frac{R_I}{R}. \tag{34}$$

It is a ratio of the internal Rayleigh number to the external one. For $\Theta \leqslant 1$, wall heating is dominant and the overall fluid layer is unstable. On the other hand, $\Theta > 1$, internal heating is dominant and a locally stable layer is formed.

Stability analysis for this problem was already made by Sparrow et al. [15]. Their interests were, however, only effects of nonlinear temperature profile on convection and they did not discuss about $\Theta$. Critical "external" Rayleigh number and critical wavenumber for each $\Theta$ changes by a selection of a characteristic temperature and a characteristic length. For instance, at $\Theta = 5$, $R_c$ calculated by using temperature difference between both boundaries and height of the fluid layer is 1463. By using the maximum temperature in the fluid layer and height of an unstable layer $L(1-h_s)$, it becomes 569 [15].

At $\Theta > 1$, convective motion may change from that of pure internal heating or that of pure wall heating. Fig. 11 shows profiles of perturbation velocity $\tilde{w}$. The profile without wall heating is symmetrical with respect to the horizontal centerline of the fluid layer. The profile with large value of $\Theta$, $\Theta = 20$, however, becomes asymmetric and the position of the maximum $\tilde{w}$ moves to upward. Therefore the center of convective motion is displaced to upward. As already mentioned in the last section, convective motion of internally heated convection is potentially asymmetric, and then a local stable layer formed near the bottom may enhance such asymmetric convective motion.

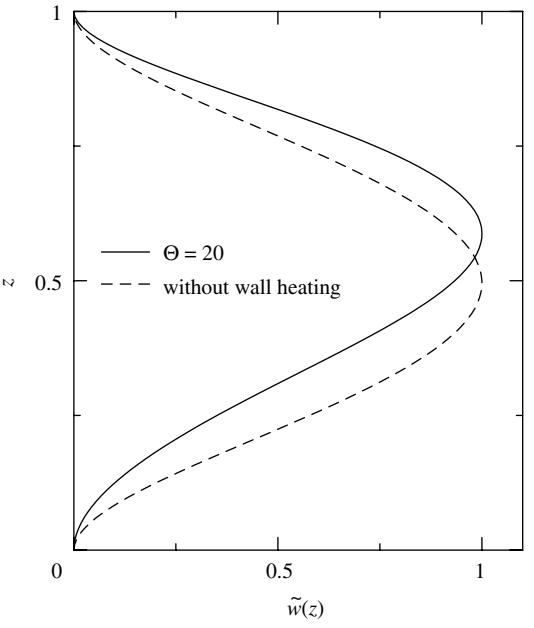


Fig. 11. Comparison of perturbation velocity profiles $\tilde{w}(z)$; soid line $\Theta = 20$ and broken line internally heated layer without wall heating.

### 4.2. With distributed internal heating

Formation of a local stable layer in the combination of internal heating and wall heating at the bottom and symmetry breaking of a profile of velocity perturbation $\tilde{w}$ were discussed. Distributed internal heating in which heat source concentrates on the top boundary makes a quasi-stable layer and also induces such a symmetry breaking as mentioned in the last section. Such distributed internal heat source may accelerate asymmetry of $\tilde{w}$ in convection which has internal heating and wall heating at the bottom. We investigate formation of a local stable layer and asymmetry of $\tilde{w}$.

Temperature profile in conduction state is derived as

$$\overline{T} = \frac{\overline{T}^* - T_1}{T_2 - T_1} = -\Theta_\eta f(z,\eta) + (\Theta_\eta - 1)z + 1, \tag{35}$$

where

$$\Theta_\eta = \frac{H_0 L^2}{\lambda(T_2 - T_1)} \frac{\eta^2}{Q(\eta)},$$

and

$$f(z,\eta) = e^{-1/\eta}\left(e^{z/\eta} + z - 1\right), \\ 0 \leqslant f(z,\eta) \leqslant 1 \quad \text{for } 0 \leqslant z \leqslant 1,\ \eta \geqslant 0.$$

This equation and parameter $\Theta_\eta$ are generalized temperature profile of Eq. (33) and generalized parameter of $\Theta$, and $\Theta_\eta$ is also an important parameter of the form of temperature profile. Fig. 12 shows temperature profile for $\Theta_\eta = 0.6$ and that for $\Theta_\eta = 1.5$, where $\eta = 0.2$. As shown in this figure, a local stable layer is not formed in the case with $\Theta_\eta = 0.6$ but is formed at $\Theta_\eta = 1.5$ in the lower part of the fluid layer. Its height $h_s$ becomes approximately half of the fluid layer although $\Theta_\eta$ is still small. It is easy to derive from Eq. (35) that

$$h_s = \eta \ln\left\{\eta[1 - e^{-1/\eta}] - \frac{\eta}{\Theta_\eta}\right\} + 1, \quad \lim_{\eta\to\infty} h_s = 1.$$

This equation shows that height of a stable layer for large $\Theta_\eta$ becomes large beyond half height of the fluid layer, which is the maximum height in uniform heating case. Such thicker stable layer enhances asymmetry of $\tilde{w}$ than in wall heating with uniform internal heating in which it needs large value of $\Theta$. For instance, at $\eta = 0.2$ and $\Theta_\eta$, the center of the circulation in which $\tilde{w}$ is the maximum moves to upward by 5% of height of the fluid layer even small value of $\Theta_\eta$.

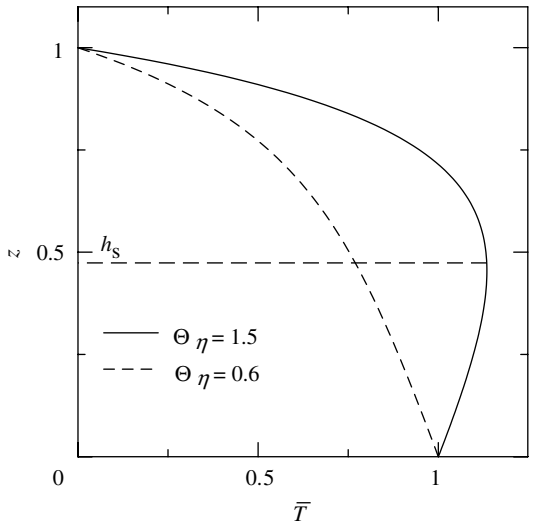


Fig. 12. Comparison of temperature profiles for difference $\Theta_\eta$ at $\eta = 0.2$; solid line $\Theta_\eta = 1.5$ and broken line $\Theta_\eta = 0.6$. $h_s$ shows height of local stable layer in which temperature gradient is positive in the vertical direction.

By substituting Eq. (35) into Eq. (16), perturbation equation becomes

$$\left(\frac{d^2}{dz^2} - k^2 - \sigma\right)\widetilde{T} = -\left\{\frac{\Theta_\eta}{\eta}\exp\left(\frac{z-1}{\eta}\right) - \Theta_\eta\left[1 - \exp\left(-\frac{1}{\eta}\right)\right] + 1\right\}\tilde{w}. \quad (36)$$

From Eq. (15),

$$\left(\frac{d^2}{dz^2} - k^2 - \frac{\sigma}{Pr}\right)\left(\frac{d^2}{dz^2} - k^2\right)\tilde{w} = Rk^2\widetilde{T}, \quad (37)$$

where this Rayleigh number is the external Rayleigh number expressed as

$$R = \frac{g\beta(T_2 - T_1)L^3}{\nu_1\kappa_1}. \quad (38)$$

Because both boundaries are isothermal, boundary conditions for temperature perturbation are

$$\widetilde{T} = 0 \quad \text{at } z = 0, 1. \quad (39)$$

Stability analysis calculated $R_c$ and $k_c$ for each $\Theta$ with $\eta = 0.2$ as shown in Fig. 13. $\Theta_\eta = 0$ means no internal heating, namely this case is the same to Rayleigh–Bénard convection. Here critical values calculated in Reid and Harris [14] are used as critical values at $\Theta_\eta = 0$. $R_c$ increases monotonically with respect to $\Theta_\eta$. When $\Theta_\eta \leqslant 1$, temperature gradient at the bottom becomes small with increase of $\Theta_\eta$, and then inflow of heat at the bottom becomes small. On the other hand, when $\Theta_\eta > 1$, reversal of temperature gradient near the bottom causes outflow of heat at the bottom. These might

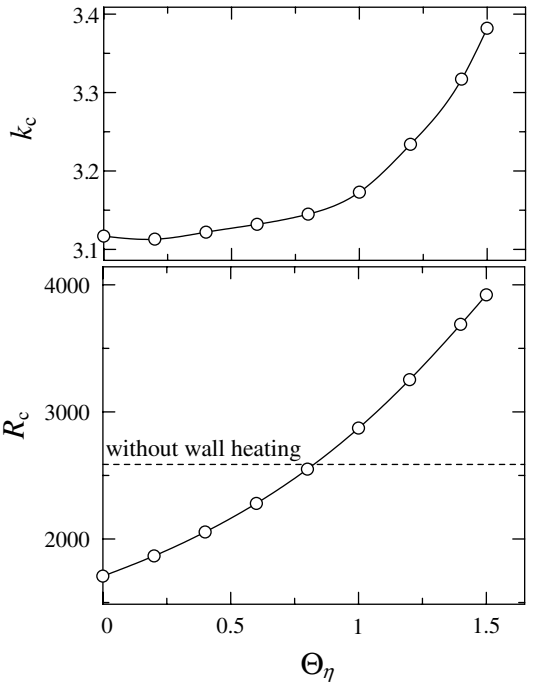


Fig. 13. Variation of critical Rayleigh number $R_c$ (below) and critical wavenumber $k_c$ (above) versus $\Theta_\eta$ at $\eta = 0.2$, broken line expresses $R_c$ for distributed internal heating with $\eta = 0.2$ without wall heating.

increase $R_c$. The slope of variation of $k_c$ with respect to $\Theta_\eta$ increases greatly from $\Theta_\eta = 1$. Therefore an increase of wavenumber may be induced by formation of a local stable layer.

## 5. Conclusions

Linear stability analysis was used to clarify the effects of heat source distribution on internally heated convection. The conditions for the onset of convection, namely the critical Rayleigh number $R_c$ and critical wavenumber $k_c$, were determined for non-uniform distributions of heat source in which heat source is concentrated in the lower or the upper part of the fluid layer. Concerning the effects of the heat source distribution a function of $R_c$ and $k_c$, (defined with respect to the characteristic length of the source distribution), the following conclusions have been drawn. Concentration of the heat source near the bottom boundary lowers $R_c$ and eases convection occurring, namely it lowers the temperature difference at which convection occurs. Variation of $k_c$, however, is small, and there is only a slight influence of this distribution on the size of the convection cell. Concentration of the heat source near the top boundary increases $R_c$ and prevents convection occurring. When

the concentration is extreme, with extremely small $\eta$, $k_c$ changes greatly in contrast to when the heat source is concentrated near the lower boundary. Furthermore, an asymmetry of the vertical velocity $\tilde{w}$ appears, and then convective flow near the bottom boundary becomes weak. These variations of the characteristics of convective motion may be caused by a quasi-stable layer formed on the lower part of the fluid layer. In common with both heat source distributions, even a slight deviation from uniform heating induces a large difference in the total power input, even though the temperature profiles are similar.

We also investigated "mixed convection" where wall heating at the bottom boundary is combined with internal heating. The dimensionless parameter $\Theta$, defined as the ratio of internal to external Rayleigh number, determines the form of the temperature profile. A local stable layer in which temperature increases in the vertical direction is formed near the bottom boundary when $\Theta$ is greater than 1, and a temperature profile similar to pure internally heated convection for $\Theta < 1$. For large values of $\Theta$ a strong asymmetry in the vertical velocity $\tilde{w}$ appears, and flow near the bottom boundary becomes weak. When the heat source distribution is non-uniform and concentrated near the upper boundary, an asymmetry appears even for small internal Rayleigh numbers; that is, small value of $\Theta_\eta$. The local stable layer formed in this case is thicker than for uniform internal heating. It spreads into the upper half of the fluid layer even for a small value of $\Theta_\eta$. Such a local stable layer might cause a large change in $R_c$ and $k_c$.

**Appendix A.** In the calculations, the region $z = [0, 1]$ is divided into some parts, and then Eq. (19) becomes

$$\tilde{w} = \sum_{i=0}^{5} C_i f^{(i)}(z-a), \quad f^{(i)} = \sum_{n=0}^{\infty} b_n^{(i)}(z-a)^n.$$

A heat source distribution function $\exp(-z/\varepsilon)$ can be expanded by Taylor series around $z = a$ as

$$\exp\left(-\frac{z}{\varepsilon}\right) = \exp\left(-\frac{a}{\varepsilon}\right)\sum_{m=0}^{\infty}\frac{(-1)^m}{m!}\left(\frac{z-a}{\varepsilon}\right)^m.$$

By assuming that the power series (26) is a solution of Eq. (25),

$$\sum_{n=0}^{\infty}\left\{\frac{n!}{(n-6)!}b_n(z-a)^{n-6} - 3k^2\frac{n!}{(n-4)!}b_n(z-a)^{n-4} + 3k^4\frac{n!}{(n-2)!}b_n(z-a)^{n-2} + \left[-\frac{R_1k^2}{C(\varepsilon)}\exp\left(-\frac{a}{\varepsilon}\right)\sum_{m=0}^{\infty}\frac{(-1)^m}{m!\varepsilon^m}(z-a)^{m+n} + \left(\frac{R_1k^2}{C(\varepsilon)} - k^6\right)(z-a)^n\right]b_n\right\} = 0.$$

For this equation to hold for all $z$, all of the series coefficients $b_n$ have to be zero. And then following recursion relation can be derived.

$$b_n = \frac{1}{n!}\left\{3k^2(n-2)!b_{n-2} - 3k^4(n-4)!b_{n-4} + \left[\left(k^6 - \frac{Ra_1k^2}{C(\varepsilon)}\right)b_{n-6} + \frac{R_1k^2}{C(\varepsilon)}\exp\left(-\frac{a}{\varepsilon}\right) \times \sum_{m=0}^{\infty}\frac{(-1)^m}{m!\varepsilon^m}b_{n-6-m}\right](n-6)!\right\} = 0.$$

In the actual calculation, cutoff number for $n$ and $m$ were 20 and 6 respectively, and the region $z = [0,1]$ was divided into 10 intervals.

## References


[1] D.P. Mckenzie, J.M. Roberts, N.O. Weiss, Convection in the earth's mantle: Toward a numerical simulation, J. Fluid Mech. 62 (1974) 465–538.

[2] S.A. Weinstein, P. Olson, Planforms in thermal convection with internal heat sources at altge Rayleigh and Plandtl numbers, Geophys. Res. Lett. 17 (1990) 239–242.

[3] B. Travis, S. Weinstein, P. Olson, Three-dimensional convection planforms with internal heat generation, Geophys. Res. Lett. 17 (1990) 243–246.

[4] D.L. Turcotte, J. Schubert, G. Schubert, Mantle Convection in the Earth and Planets, Cambridge Univ. press, Cambridge, 2001.

[5] D.J. Tritton, Internally heated convection in the atmosphere of Venus and in the laboratory, Nature 257 (1975) 110–112.

[6] R. Krishnamurti, Convection induced by selective absorption of radiation: A laboratory model of conditional instability, Dyn. Atmos. Oceans 27 (1997) 367–382.

[7] D.J. Tritton, M.N. Zarraga, Convection in horizontal layers with internal heat generation: Experiments, J. Fluid Mech. 30 (1967) 21–32.

[8] E.W. Schwiderski, H.J.A. Schwab, Convection experiments with electrolytically heated fluid layers, J. Fluid Mech. 48 (1971) 703–719.

[9] P.H. Roberts, Convection in horizontal layers with internal heat generation: Theory, J. Fluid Mech. 30 (1967) 33–49.

[10] M. Tveitereid, E. Palm, Convection due to internal heat sources, J. Fluid Mech. 76 (1976) 481–499.

[11] M. Tveitereid, Thermal convection in a horizontal fluid layer with internal heat sources, Int. J. Heat Mass Transfer 21 (1978) 335–339.

[12] Y. Tasaka, K. Yonekura, Y. Kudo, Y. Takeda, T. Yanagisawa, Dilatation of Convection Cell in the Natural Convection induced by Internal Heating, Phys. Fluids., in press.

[13] A. Yücel, Y. Bayazitoglu, Onset of convection in fluid layers with non-uniform volumetric energy sources, Trans. ASME, J. Heat Transfer 101 (1979) 666–671.

[14] W.H. Reid, D.L. Harris, Some further results on the Bénard problem, Phys. Fluids 1 (1958) 102–110.

[15] E.M.R. Sparrow, R.J. Goldstein, V.K. Jonsson, Thermal instability in a horizontal fluid layer: Effect of boundary conditions and non-linear temperature profile, J. Fluid Mech. 18 (1964) 513–528.

[16] F.A. Kulacki, R.J. Goldstein, Hydrodynamic instability in fluid layers with uniform volumetric energy sources, Appl. Scientific Res. 31 (1975) 81–109.